

# Synthesis and Characterization of Inorganic–Organic Hybrid Gallium Selenides

Sarah J. Ewing<sup>†</sup> and Paz Vaqueiro<sup>\*,†,‡</sup>

<sup>†</sup>Institute of Chemical Sciences, Heriot Watt University, Edinburgh EH14 4AS, U.K.

## Supporting Information

**ABSTRACT:** Two semiconducting hybrid gallium selenides,  $[\text{Ga}_6\text{Se}_9(\text{C}_6\text{H}_{14}\text{N}_2)_4][\text{H}_2\text{O}]$  (**1**) and  $[\text{C}_6\text{H}_{14}\text{N}_2]_2[\text{Ga}_4\text{Se}_6(\text{C}_6\text{H}_{14}\text{N}_2)_2]$  (**2**), were prepared using a solvothermal method in the presence of 1,2-diaminocyclohexane (1,2-DACH). Both materials consist of neutral inorganic layers, in which 1,2-DACH is covalently bonded to gallium. In **1**, the organic amine acts as a monodentate and a bidentate ligand, while in **2**, bidentate and uncoordinated 1,2-DACH molecules coexist.

Condensed gallium chalcogenides, prepared by conventional solid-state synthesis, have been the subject of numerous studies, owing to their interesting semiconducting and nonlinear optical properties.<sup>1</sup> By contrast, the development of microporous and hybrid gallium chalcogenides, especially selenides and tellurides, is still in its early stages. Solvothermal synthesis has been successfully exploited for the preparation of gallium sulfide and selenide frameworks consisting of corner-linked supertetrahedral clusters.<sup>2</sup> These framework materials exhibit high surface areas, ion-exchange capacity, and photoluminescence. In the case of gallium sulfides, organic amines can act as linkers between supertetrahedral clusters, leading to the formation of a variety of hybrid one-, two-, and three-dimensional covalent networks.<sup>3</sup> Supertetrahedral clusters appear to be less prevalent in gallium selenide chemistry, and the formation of organically functionalized tetrahedral clusters has not been reported to date. Moreover, solvothermally prepared gallium selenides in which amines are covalently bonded to the anionic network are extremely rare, with only one example known,  $[\text{enH}][\text{Ga}_4\text{Se}_7(\text{en})_2]$ .<sup>4</sup> Here we report the crystal structure (Table 1) and optical properties of two hybrid gallium selenides,  $[\text{Ga}_6\text{Se}_9(\text{C}_6\text{H}_{14}\text{N}_2)_4][\text{H}_2\text{O}]$  (**1**) and  $[\text{C}_6\text{H}_{14}\text{N}_2]_2[\text{Ga}_4\text{Se}_6(\text{C}_6\text{H}_{14}\text{N}_2)_2]$  (**2**), which were prepared under solvothermal conditions (see the Supporting Information, SI), in the presence of 1,2-diaminocyclohexane (1,2-DACH). The ability of this amine to act as a chelating ligand leads to products markedly different from those previously found by us using the 1,4-diaminocyclohexane isomer.<sup>5</sup>

The crystal structure of **1** (Table 1) contains four crystallographically independent gallium atoms (Figure 1), found in

either solely inorganic  $\text{GaSe}_4$  tetrahedra or in hybrid tetrahedra,  $\text{GaSe}_3\text{N}$  and  $\text{GaSe}_2\text{N}_2$ , in which 1,2-DACH acts as a monodentate or a bidentate ligand, respectively. Ga–Se distances range from 2.3148(10) to 2.4233(9) Å, which are comparable to Ga–Se distances in gallium selenides in the literature,<sup>4</sup> while Ga–N distances, which range from 2.018(12) to 2.030(6) Å, are significantly shorter than the Ga–Se distances.

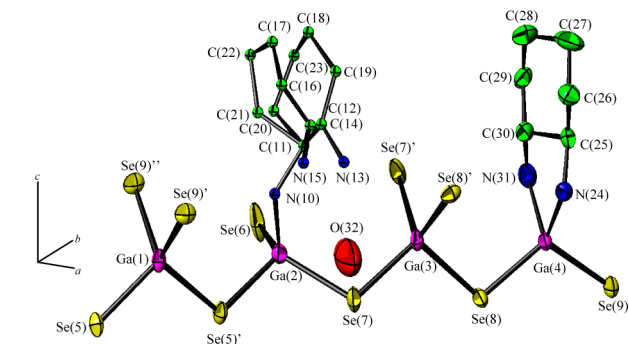


**Figure 1.** Local coordination diagram for **1** showing the atom-labeling scheme and ellipsoids at 50% probability.

The structure of **1** contains chains of vertex-sharing tetrahedra, in which  $\text{GaSe}_4$  tetrahedra alternate with  $\text{GaSe}_3\text{N}$  and  $\text{GaSe}_2\text{N}_2$  tetrahedra. Cross-linking of these chains through the terminal selenium atoms results in the formation of layers containing 8- and 6-membered rings (Figure 2a). These layers, which are neutral, are aligned parallel to the (001) plane and arranged in a *back-to-back* stacking sequence (Figure 2b), with the ligands rotated by ca. 90° on opposite sides of consecutive layers.

The monodentate 1,2-DACH ligand is disordered over two positions, which correspond to the *cis* and *trans* isomers (Figure 1). The *cis* isomer is dominant with a 65(1)% occupancy compared to 35(1)% for the *trans* isomer. A water molecule is located inside each 8-membered ring, and the distances between noncoordinating amine groups and water  $[\text{N}(13)\text{--}cis\text{-O } 2.75(4)]$

Received: May 15, 2014  
Published: August 12, 2014

**Table 1.** Crystallographic Data for **1** and **2**

	<b>1</b>	<b>2</b>
cryst syst	orthorhombic	monoclinic
space group	<i>Pnma</i>	<i>P2<sub>1</sub>/n</i>
<i>a</i> /Å	11.1919(7)	14.2095(8)
<i>b</i> /Å	19.6774(12)	11.0633(6)
<i>c</i> /Å	20.8361(13)	21.2998(11)
$\beta$ /deg		105.253(3)
no. of param refined	191	211
$R_{\text{merg}}$	0.080	0.054
$R [I > 3\sigma(I)]$	0.0369	0.0550
$R_w$	0.0385	0.0530

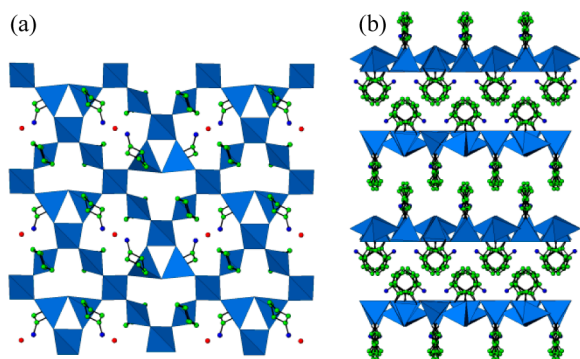


**Figure 2.** Views of (a) a  $[\text{Ga}_4\text{Se}_6(\text{C}_6\text{H}_{14}\text{N}_2)_4]$  layer along  $[001]$  and (b) the crystal structure of **1** along  $[210]$ .

$\text{Å}$ ;  $\text{N}(15)\text{--}trans\text{-O } 2.60(3) \text{ Å}$ ] are consistent with the presence of hydrogen-bonding interactions.

The structure of **2** contains neutral  $[\text{Ga}_4\text{Se}_6(\text{C}_6\text{H}_{14}\text{N}_2)_2]$  layers, in which 1,2-DACH acts as a bidentate ligand. These layers are composed of chains of alternating  $\text{GaSe}_4$  and  $\text{GaSe}_2\text{N}_2$  tetrahedra (Figure 3). In these tetrahedra, Ga–Se distances lie

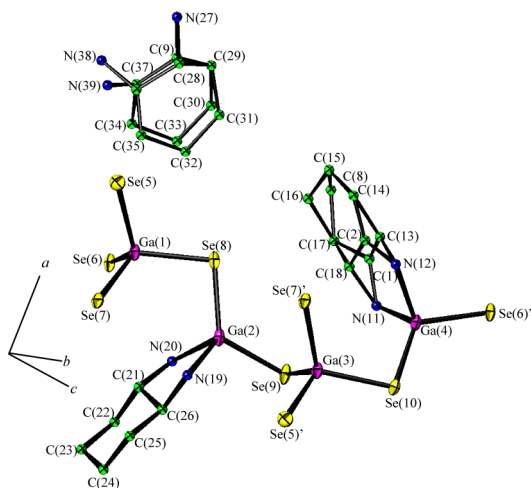


**Figure 3.** Local coordination diagram for **2** showing the atom-labeling scheme and ellipsoids at 50% probability.

over the range  $2.3108(13)\text{--}2.4203(11) \text{ Å}$ , while Ga–N distances range from  $2.016(7)$  to  $2.040(7) \text{ Å}$ . These are comparable to values in the literature<sup>4</sup> and to those found for **1**.

Within a given a chain, the  $\text{GaSe}_4$  and  $\text{GaSe}_2\text{N}_2$  tetrahedra are linked by their corners. Additional edge-sharing linkages through the terminal Se(5) and Se(7) create layers, which contain 6- and 14-membered rings (Figure 4a). The inorganic component of the layer has a sinusoidal-wave shape, while the bidentate 1,2-DACH ligands are oriented toward the outer part of the layers. The layers are stacked in an AB repeating sequence, with additional 1,2-DACH moieties located between the layers. Because the layers are neutral, protonation of the uncoordinated 1,2-DACH molecules is not required. Both cis and trans isomers are present in the crystal structure. The interlayer 1,2-DACH is a 51(2):49(2) cis/trans mixture, while the bidentate 1,2-DACH bonded to Ga(4) is a 41(2):59(2) cis/trans mixture. The N–H $\cdots$ Se distances between the noncoordinating 1,2-DACH and the layers [e.g.,  $\text{N}(27)\text{--}\text{Se}(9) 3.501(7) \text{ Å}$ ] imply the presence of hydrogen-bonding interactions.

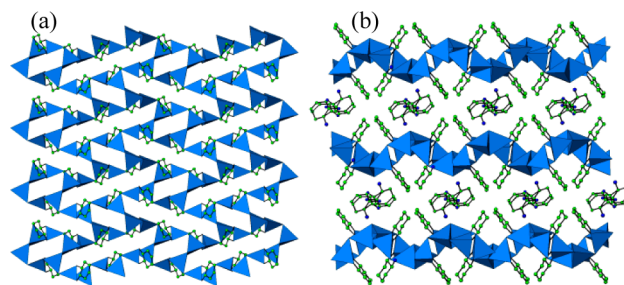


**Figure 4.** Views of (a) a layer of **2** along  $[30\bar{1}]$  and (b) the crystal structure of **2** along  $[010]$ .

IR spectra (see the SI) of **1** and **2** are consistent with the presence of 1,2-DACH. Stretches at  $3138$  and  $3204 \text{ cm}^{-1}$  for **1** and **2**, respectively, can be assigned to the N–H symmetric stretch of the  $\text{--NH}_2$  groups. Peaks at  $2962$  and  $2897 \text{ cm}^{-1}$  for **1** and **2**, respectively, were assigned to C–H stretches. C–N stretching vibrations are observed at  $1396$  and  $1378 \text{ cm}^{-1}$  for **1** and **2**, respectively.

Thermogravimetric analysis (TGA; see the SI) under an oxidizing atmosphere shows that **1** and **2** are stable up to ca.  $150$  and  $200 \text{ °C}$ , respectively. Decomposition of the materials occurs in two steps. A  $\sim 20\%$  weight loss is observed for the initial decomposition step of **1**. This weight change could be attributed to the loss of water and monodentate 1,2-DACH (calcd  $15.5\%$ ). The overall weight loss is  $65.1\%$ , in excellent agreement with the calculated weight loss of  $64.9\%$  for the decomposition of **1** to  $\text{Ga}_2\text{O}_3$ . The first decomposition step of **2**,  $26.2\%$ , can be attributed to the loss of the 1,2-DACH moieties (calcd  $31.3\%$ ). A total loss of  $59.9\%$  is in reasonable agreement with the decomposition of **2** to  $\text{Ga}_2\text{O}_3$  (calcd  $65.8\%$ ).

The UV–vis optical absorption spectra of **1** and **2** are shown in Figure 5. The estimated band gaps are  $2.36(2) \text{ eV}$  for **1** and

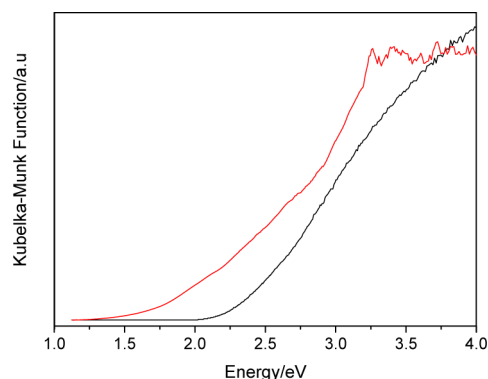


**Figure 5.** Optical absorption spectra of **1** (black line) and **2** (red line).

$2.30(6) \text{ eV}$  for **2**, larger than those found for the bulk selenides  $\text{Ga}_2\text{Se}_3$  ( $2.1 \text{ eV}$ ) and  $\text{GaSe}$  ( $1.97 \text{ eV}$ ).<sup>6</sup> For solvothermally prepared antimony sulfides, it has been found that an increase in the framework density leads to a decrease in the optical band gap.<sup>7</sup> This correlation also seems to hold here, given that **1** and **2** have larger band gaps than the corresponding condensed phases. This is consistent with density functional theory calculations on a related layered hybrid selenide,  $[\text{CdSe}(\text{hda})_{0.5}]$  (hda = 1,6-hexanediamine), which shows that the electronic band-edge states are dominated by the inorganic layers and that the conduction and valence bands are narrower than those in bulk CdSe, resulting in a larger band gap.<sup>8</sup>

An unusual feature of **1** and **2** is the presence of an organic amine covalently bonded to a main-group metal center. In solvothermally prepared main-group chalcogenides, the organic amines are normally incorporated into the crystal structure as counteranions and bonded through electrostatic and weak hydrogen-bonding interactions.<sup>9</sup> Gallium, however, has a higher acid character than other main-group elements, and this favors bonding with hard bases, in this case the organic amine. Covalently bonded amines have been previously found in gallium sulfides<sup>3</sup> and in  $[\text{enH}][\text{Ga}_4\text{Se}_7(\text{en})_2]$ .<sup>4</sup> In the heavier tellurides, amines have been found to form covalent bonds to indium, as exemplified by  $[\text{M}(\text{phen})_3]_2[\text{In}_{18}\text{Te}_{30}(\text{dapn})_6] \cdot 2\text{Hdapn} \cdot \text{dapn}$  ( $\text{M} = \text{Fe}^{\text{II}}$ , and  $\text{Ni}^{\text{II}}$ ;  $\text{dapn} = 1,3\text{-diaminopropane}$ ),<sup>10</sup>  $[\text{Mn}(\text{DACH})_3]_2[\text{In}_{18}\text{Te}_{30}(\text{DACH})_6][\text{DACHH}_2][\text{H}_2\text{O}]$ ,<sup>11</sup> and  $[\text{In}(\text{en})_3][\text{In}_3\text{Te}_8(\text{en})_2] \cdot 0.5\text{en}$ .<sup>12</sup> This suggests that for group 13 elements the relative stabilities of the metal–chalcogen and metal–nitrogen bonds under solvothermal conditions are finely balanced.

The hybrid gallium selenides reported here can be considered to be related to the family of II/VI hybrid semiconductors, which have the general formula  $[\text{MQ}(\text{L})_x]$  ( $\text{M} = \text{Mn}, \text{Zn}, \text{Cd}$ ;  $\text{Q} = \text{S}, \text{Se}, \text{Te}$ ;  $\text{L} = \text{organic amine}$ ), and consist of inorganic slabs sandwiched by covalently bonded organic layers.<sup>13</sup> These hybrid materials have been found to exhibit remarkable properties, including large-band-gap tunability,<sup>13</sup> broad photoluminescent emission, which can result in direct white-light emission,<sup>13c,e</sup> and zero thermal expansion.<sup>13b</sup> The inorganic slabs of the  $[\text{MQ}(\text{L})_x]$  phases retain the connectivity of the zinc blende or wurtzite structures found in bulk II/VI semiconductors and consist of corner-sharing  $\text{MQ}_4$  and  $\text{MQ}_3\text{N}$  tetrahedra. By contrast, the inorganic layers in **1** and **2** are not related to the defect zinc blende structure of  $\text{Ga}_2\text{Se}_3$  and contain  $\text{GaSe}_4$ ,  $\text{GaSe}_3\text{N}$ , and  $\text{GaSe}_2\text{N}_2$  tetrahedra, which can be vertex- or edge-linked. However, in common with  $[\text{MQ}(\text{L})_x]$  phases, the layers in **1** and **2** are neutral and are held together by weak van der Waals or hydrogen-bonding interactions. It has been shown that exfoliation of  $[\text{MQ}(\text{L})_x]$  phases is possible and results in the creation of free-standing single layers,<sup>14</sup> which can be considered inorganic graphene analogues. We envisage that exfoliation of **1** and **2** may also be feasible. Our current efforts with hybrid gallium selenides are directed toward the synthesis of additional members of this family and the detailed investigation of their optical properties.

## ■ ASSOCIATED CONTENT

### ■ Supporting Information

Experimental procedures, crystallographic data in CIF format, powder X-ray diffraction data, elemental analysis, Fourier transform infrared spectra, and TGA data. This material is available free of charge via the Internet at <http://pubs.acs.org>.

## ■ AUTHOR INFORMATION

### Corresponding Author

\*E-mail: [p.vaqueiro@reading.ac.uk](mailto:p.vaqueiro@reading.ac.uk)

### Present Address

‡P.V.: Department of Chemistry, University of Reading, Whiteknights, Reading RG6 6AD, U.K.

### Notes

The authors declare no competing financial interest.

## ■ ACKNOWLEDGMENTS

S.J.E. thanks Heriot Watt University for studentship. The authors thank Christina Graham for elemental analysis data.

## ■ REFERENCES

- (1) (a) Panich, A. M. *J. Phys.: Condens. Matter* **2008**, *20*, 293202. (b) Johnsen, S.; Liu, Z.; Peters, J. A.; Song, J.-H.; Peter, S. C.; Malliakas, C. D.; Cho, N. K.; Jin, H.; Freeman, A. J.; Wessels, B. W.; Kanatzidis, M. G. *Chem. Mater.* **2011**, *23*, 3120–3128. (c) Fernelius, N. C. *Prog. Cryst. Growth Charact. Mater.* **1994**, *28*, 275–353. (d) Tell, B.; Kasper, H. M. *Phys. Rev. B* **1971**, *4*, 4455–4459. (e) Contreras, M. A.; Egaas, B.; Ramanathan, K.; Hiltner, J.; Swartzlander, A.; Hasoon, F.; Noufi, R. *Prog. Photovoltaics* **1999**, *7*, 311–316.
- (2) (a) Zheng, N.; Bu, X.; Wang, B.; Feng, P. *Science* **2002**, *298*, 2366–2369. (b) Zheng, N.; Bu, X.; Feng, P. *J. Am. Chem. Soc.* **2003**, *125*, 1138–1139. (c) Vaqueiro, P.; Romero, M. L. *J. Phys. Chem. Solids* **2007**, *68*, 1239–1243. (d) Wu, T.; Wang, X.; Bu, X.; Zhao, X.; Wang, L.; Feng, P. *Angew. Chem., Int. Ed.* **2009**, *48*, 7204–7207.
- (3) (a) Vaqueiro, P.; Romero, M. L. *J. Am. Chem. Soc.* **2008**, *130*, 9630–9631. (b) Vaqueiro, P.; Romero, M. L. *Inorg. Chem.* **2009**, *48*, 810–812. (c) Vaqueiro, P.; Romero, M. L.; Rowan, B. C.; Richards, B. S. *Chem.—Eur. J.* **2010**, *16*, 4462–4465. (d) Wu, T.; Khazhaky, R.; Wang, L.; Bu, X.; Zheng, S.-T.; Chau, V.; Feng, P. *Angew. Chem., Int. Ed.* **2011**, *50*, 2536–2539.
- (4) Dong, Y.; Peng, Q.; Wang, R.; Li, Y. *Inorg. Chem.* **2003**, *42*, 1794–1796.
- (5) (a) Ewing, S. J.; Powell, A. V.; Vaqueiro, P. *J. Solid State Chem.* **2011**, *184*, 1800–1804. (b) Ewing, S. J.; Romero, M. L.; Hutchinson, J.; Powell, A. V.; Vaqueiro, P. *Z. Anorg. Allg. Chem.* **2012**, *638*, 2526–2531.
- (6) (a) Springford, M. *Proc. Phys. Soc.* **1963**, *82*, 1020–1028. (b) Bube, R. H.; Lind, E. L. *Phys. Rev.* **1959**, *115*, 1159–1164.
- (7) Powell, A. V.; Lees, R. J.; Chippindale, A. M. *J. Phys. Chem. Solids* **2008**, *69*, 1000–1006.
- (8) Wei, S.; Lu, J.; Qian, Y. *Chem. Mater.* **2008**, *20*, 7220–7227.
- (9) (a) Sheldrick, W. S. *J. Chem. Soc., Dalton Trans.* **2000**, 3041–3052. (b) Sheldrick, W. S.; Wachhold, M. *Coord. Chem. Rev.* **1998**, *176*, 211–322. (c) Powell, A. V. *Int. J. Nanotechnol.* **2011**, *8*, 783–794.
- (10) Zhang, X.; Pu, Y.-Y.; You, L.-S.; Bian, G.-Q.; Zhu, Q.-Y.; Dai, J. *Polyhedron* **2013**, *52*, 645–649.
- (11) Wang, Y.-H.; Luo, W.; Jiang, J.-B.; Bian, G.-Q.; Zhu, Y.-Q.; Dai, J. *Inorg. Chem.* **2012**, *51*, 1219–1221.
- (12) Zhang, Q. C.; Chung, I.; Jang, J. I.; Ketterson, J. B.; Kanatzidis, M. G. *Chem. Mater.* **2009**, *21*, 12–14.
- (13) (a) Huang, X.; Li, J.; Fu, H. *J. Am. Chem. Soc.* **2000**, *122*, 8789–8790. (b) Zhang, Y.; Islam, Z.; Ren, Y.; Parilla, P. A.; Ahrenkiel, S. P.; Lee, P. L.; Mascarenhas, A.; McNevin, M. J.; Naumov, I.; Fu, H.-X.; Huang, X.-Y.; Li, J. *Phys. Rev. Lett.* **2007**, *99*, 215901. (c) Ki, W.; Li, J. *J. Am. Chem. Soc.* **2008**, *130*, 8114–8115. (d) Huang, X.; Roushan, M.; Emge, T. J.; Bi, W.; Thiagarajan, S.; Cheng, J.-H.; Yang, R.; Li, J. *Angew. Chem., Int. Ed.* **2009**, *48*, 7871–7874. (e) Ki, W.; Li, J.; Eda, G.; Chhowalla, M. *J. Mater. Chem.* **2010**, *20*, 10676–10679. (f) Huang, X.; Li, J. *J. Am. Chem. Soc.* **2007**, *129*, 3157–3162.
- (14) Sun, Y.; Sun, Z.; Gao, S.; Cheng, H.; Liu, Q.; Piao, J.; Tao, T.; Wu, C.; Hu, S.; Wei, S. *Nat. Commun.* **2012**, *3*, 1057.